CHAPTER 1

INTRODUCTION

CHAPTER 1

INTRODUCTION

1.1. An Origin of High Power Microwave (HPM) Source

In the 1940s, the US military tested an atmospheric nuclear explosion, and after this explosion, scientists noticed electrical black-outs in the electronics equipment there. Scientists concluded that the reason behind the electrical black-out in electronics devices was the high-power electromagnetic pulse (EMP), which was generated by the nuclear explosion. If such a pulse could be generated without any nuclear explosion then it can be used as a non-lethal weapon that can destroy or disturb the electronics circuits or components or devices rather than damaging the infrastructure or harming people. This was the prime idea behind the origin of HPM [Abrams (2003)].

1.2. Definition of HPM Source

The HPM is an inexplicit term used by many research communities that study the generation of coherent electromagnetic (EM) radiation. The general definition for the HPM is [Barker and Schamiloglu (2001), Benford *et al.* (2007)]:

- Devices that operate in the centimeter and millimeter-wave range (i.e. frequency between 1 to 300 GHz).
- Devices that generate a minimum RF power of 100 MW, or
- RF energy of more than 1 kJ.

1.3. Classification of HPM Source

There are several ways to classify the HPM sources, but the most prominent and accepted ways are [Barker and Schamiloglu (2001), Benford *et al.* (2007)]:

- Phase velocity (i.e. Slow-wave or Fast-wave devices)
- Electrons participation in the coherent EM generation process
- According to the generated RF pulse width
- According to the generated RF power

Most microwave tubes are based on the principle of converting the kinetic energy of the electron beam into coherent electromagnetic radiation. This conversion is possible due to the resonant interactions between the normal modes of the waveguide or cavities and the natural oscillation modes of the electron beam. From the perspective of the electromagnetic normal modes, the HPM sources are classified into either slow-wave or fast-wave devices. Slow-wave devices are those devices in which the phase velocity of the electromagnetic modes (i.e. cavities interaction mode) is less than the speed of light while in the case of fast-wave devices, the phase velocity of the electromagnetic modes (i.e. waveguide interaction mode) is greater than the speed of light.

The second way to classify the HPM sources is based on the perspective of the electrons participation in the microwave generation process, and according to this the devices are classified as follows:

- O-Type
- M-Type
- Space-Charge

Table 1.1. Different ways to classify the HPM source [Benford *et al.* (2007)].

Classification	**Slow-wave**	**Fast-wave**
O-Type	Relativistic- klystron oscillator (RKO). Relativistic-backward wave oscillator (RBWO). Relativistic-Transit Time Oscillator (RTTO). Surface-wave Oscillator. Multi-wave Cerenkov Generator. Dielectric Cerenkov Maser. Plasma Cerenkov Maser. Grid-less Reltron.	Free Electron Laser (FEL) Optical Klystron Gyrotron Gyro-BWO Gyro Klystron Cyclotron Auto Resonance Maser
M-Type	Relativistic Magnetron. MILO	Rippled Field Magnetron
Space-Charge	VIRCATOR. Gridded Reltron. Reflex Triode.	

In O-type devices, electrons move parallelly to an externally applied magnetic field. This externally applied magnetic field helps guide the intense electron beams used in the HPM source, and in some instances, it plays an essential role in the microwave generation process. In the second type of devices i.e. in M-type devices, electrons move perpendicularly to the crossed electric and magnetic fields. The third one is the space-charge device in which the interaction creating microwaves is inherently identifiable to an intense space-charge interaction. Such devices may operate with an external magnetic field or having self-magnetic insulation.

The third way to classify HPM sources is based on the perspective of the RF power pulse width generated from the device i.e. narrow-band or wide-band. In the narrow-band devices, the generated RF energy is concentrated in a small frequency band while in the case of the wide-band device the RF energy is distributed over a large frequency range.

The fourth way to classify the HPM source is based on the capabilities to generate the RF power, i.e. the source is either a high-peak-power HPM source or a high-average-power HPM source. A high-peak-power source implies that it generates an RF power for a very short duration (i.e. below a few hundred nanoseconds) and this source may be a single-shot or of low repetition rate. The high-average-power device means that it generates an RF power for a long duration (i.e. more than a few thousand nanoseconds) that the source is of high repetition rate. All possible ways to classifying the HPM sources discussed above are summarized in tabular form and are shown in Table 1.1.

1.4. Side-Coupled Cavity

The side-coupled cavity (SCC) finds its application as a slow-wave RF interaction cavity in linear accelerators and reltron oscillators. The linear accelerators are widely used in various domains, such as in the medical field (for cancer treatment), high power collider, food industry (food and material processing), security application (cargo inspection and baggage screening machines), nuclear physics, nuclear waste management (radioisotope production) and others [Knapp *et al.* (1965), Knapp (1976), Amaldi (1999), Miller (2006), Benford *et al.* (2007), Hamm *et al.* (2012)].

Any RF interaction structure used for the beam wave interaction in an accelerator must meet two basic requirements: (i) the value of its shunt impedance should be highest over one period, and (ii) for any given input power its gradient value should be maximum [Schächter (2011)]. The linear accelerators are mainly classified into two groups: (i) standing-wave accelerator and (ii) traveling-wave accelerator. The most popular RF interaction cavity in the linear accelerator is a periodic two-gap resonator structure (i.e. a periodic disc loaded circular waveguide structure) which is shown in Fig. 1.1. Fig. 1.1 (a) shows the two-gap resonant structure while Fig. 1.1 (b) shows the seven coupled cavities LINAC resonator structure. The normalized axial electric fields associated with different modes in the seven coupled cavities LINAC resonator structure has been shown in Fig. 1.2.

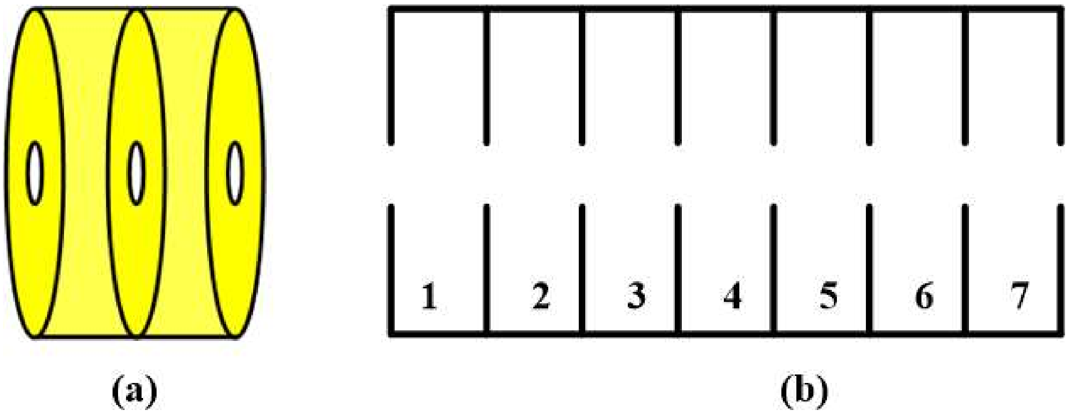

Figure 1.1: Periodic disc loaded circular waveguide structure: (a) shows the two-gap resonant structure and (b) seven coupled cavities LINAC resonator structure.

The structure operates either in a standing-wave type accelerator (i.e. π-mode configuration) or traveling-wave type accelerator (i.e. 2π/3-mode configuration) [Schächter (2011)]. These mode configurations have their unique advantages such that the 2π/3-mode configuration has the highest shunt impedance value over a period, while the π-mode configuration has the maximum gradient value for any given input power. Before selecting one of these modes as the operational mode, we must also consider the perspective of the electron and EM fields.

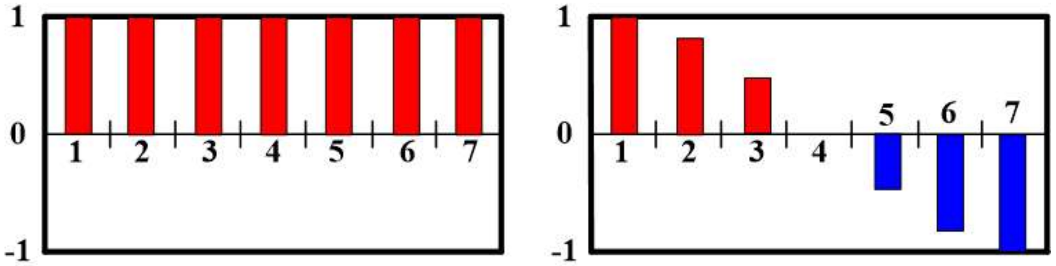

(a) 0-mode

(b) π/6-mode

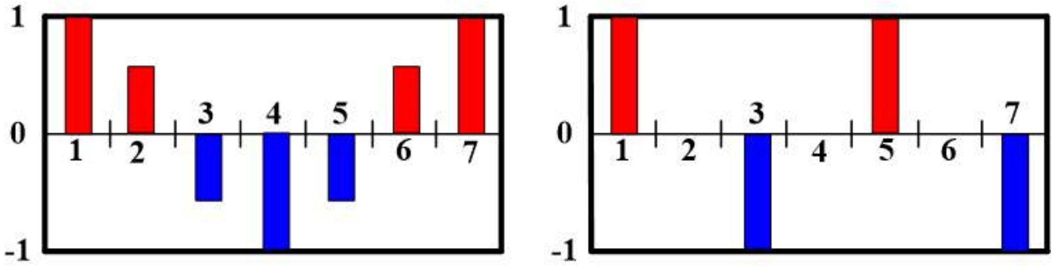

(c) π/3-mode

(d) π/2-mode

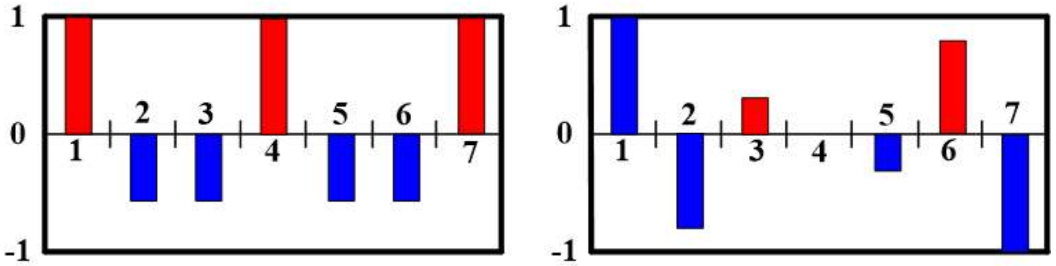

(e) 2π/3-mode

(f) 5π/6-mode

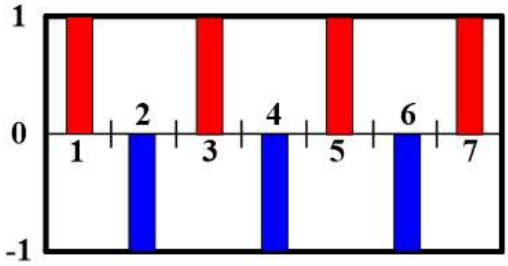

(g) π-mode

Figure 1.2: The normalized axial electric fields associated with different modes in the seven coupled cavities LINAC resonator structure [Miller (2006)].

According to the electron's perspective, the best option for operation is the standing-wave configuration (i.e. π-mode), because the gradient value is the maximum for any input power for this configuration. While the EM field's perspective completely rejects the π-mode configuration because; (i) at this point the value of the group velocity becomes zero, (ii) the presence of many close longitudinal modes near the crest of dispersion destabilizes the π-mode, and (iii) if the structure is long enough then the filling time is also long. From the EM field's perspective, the best option is the π/2-mode configuration, because in this configuration the value of group velocity has high. But for this configuration, half of the structure does not participate in acceleration that is seen through Fig. 1.2 (d), resulting in the acceleration structure being automatically lengthened, and the filling time inherently increases [Schächter (2011)].

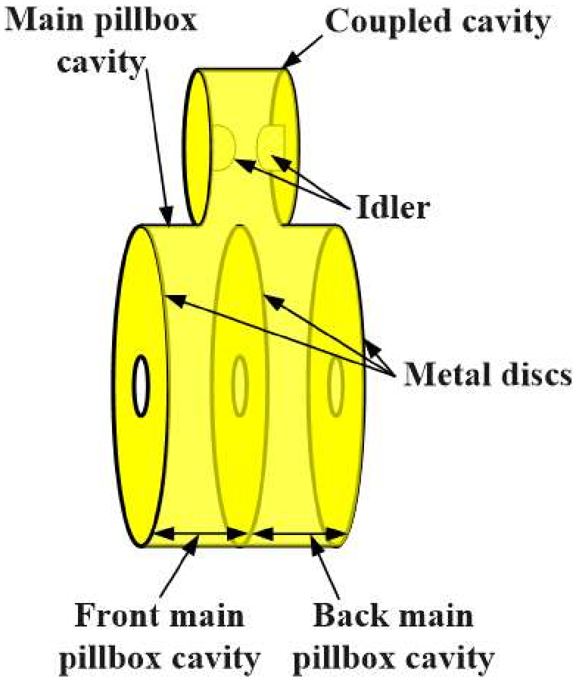

Figure 1.3: Typical geometry of SCC.

This vicious cycle was broken by Knapp *et al.* by proposing the SCC structure and this structure satisfies both perspectives i.e. electron's and EM's perspective [Knapp *et al.* (1968)]. The typical geometry of the unit cell of the SCC structure is shown in Fig. 1.3, which consists of one coupled cavity, one main pillbox cavity, and three metal discs. The metal discs are placed at the front, middle, and end of the main pillbox cavity. The metal disc placed in the middle of the main pillbox cavity segregates the main pillbox cavity into two identical cavities, known as the front and back main pillbox cavity. In SCC, the coupled-cavity mounted at the periphery of the main pillbox cavity is used to provide a magnetic coupling between the adjacent main pillbox cavities. The hole in the center of the metal disc for the beam passage provides the electric coupling between the adjacent main pillbox cavities. This multi-cavity resonating system resonates at three modes i.e. 0-mode, π/2-mode, and π-mode. The desired mode for operation in all these three modes is π/2-mode since it is the only unstable mode [Miller *et al.* (1992), Knapp *et al.* (1968)]. In the case of π/2-mode, the magnitude of the electric field present in the coupled cavity is nearly zero, while the magnitude of the electric field present in the adjacent main pillbox cavities are equal but having a phase difference of 180°. Therefore, when these electrons pass through the SCC, they experience both types of electric fields i.e. the accelerated and decelerated field similar to the π-mode of the two-gap resonant structure, and thus it fulfills the electron's perspective, whereas the SCC cavity introduced the phase difference of the π/2 radian and thus satisfied the EM's perspective. The SCC attracts the researcher due to its low sensitivity to the frequency deviation and cell-to-cell phase deviation along with a higher dimensional tolerance than the π-mode and 2π/3-mode [Nepal *et al.* (1991)]. Also, the SCC has a potential structure as an RF interaction cavity in transit time oscillator, backward wave oscillator, and traveling wave tubes. Therefore the different aspects i.e. EM and RF behavior of the SCC must be investigated.

1.5. Reltron

Presently, many HPM sources are derived from conventional microwave tubes such as relativistic backward wave oscillator (RBWO), relativistic Magnetron, relativistic klystron oscillator (RKO), relativistic transit time oscillator (RTTO). Also, some dedicated HPM sources have been developed such as VIRCATOR, MILO, Reltron, etc. All these HPM sources are typically based on explosive emission cathodes and capable of generating pulsed microwave power ranging from several hundred MW to several gigawatts. All these sources are capable of generating very high microwaves, but the major constraint associated with these sources is the width of the RF pulse which is less than 100 ns [Benford *et al.* (2007)].

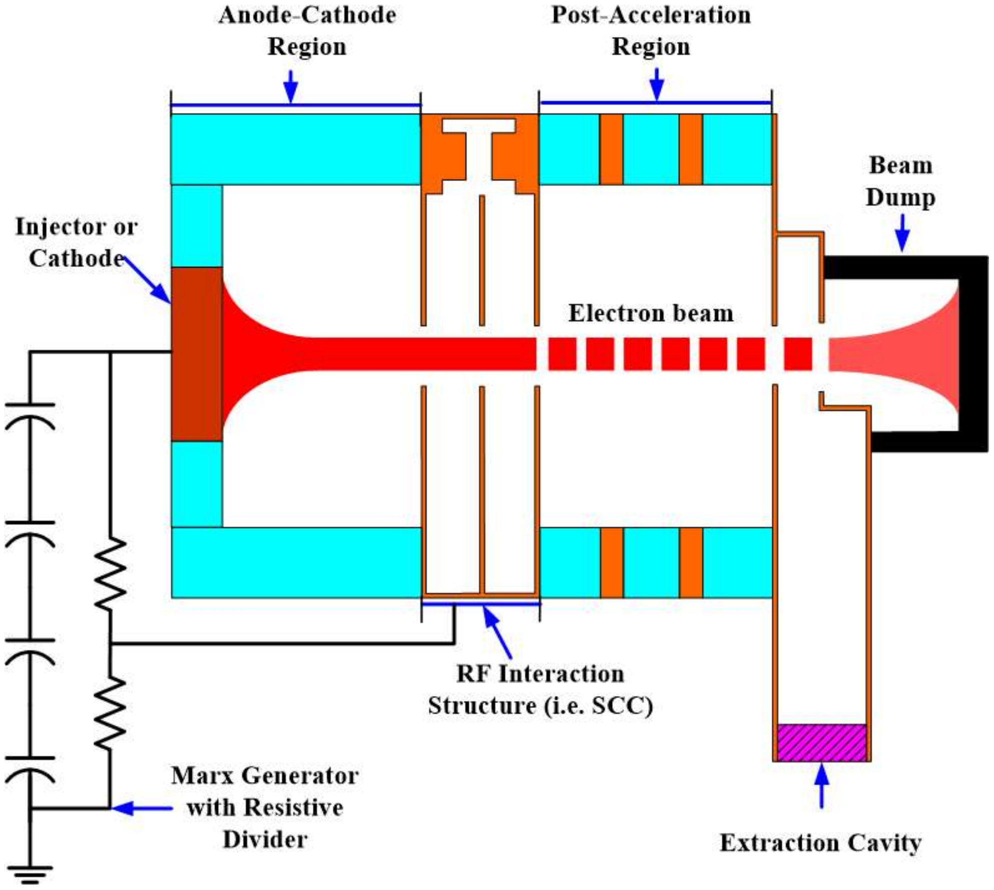

Figure 1.4: Schematic of the reltron system [Miller *et al.* (1992)].

In 1992, Titan Advanced Innovative Technologies of Albuquerque developed an HPM source Reltron as a compact, flexible, reliable, tunable, and highly efficient slow-wave microwave oscillator. The typical schematic of a reltron system is shown in Fig. 1.4. The attractive feature of Reltron is its excellent electron bunching mechanism, the post-acceleration technique used to reduce the relative velocity spread between electron bunches, and efficient microwave extraction directly in TE_{10} mode without any external mode converter [Miller *et al.* (1992)]. For the beam-wave interaction, the highly efficient reltron oscillator uses the SCC as an RF interaction cavity [Miller *et al.* (1992)]. The SCC structure as a beam wave interaction structure has several advantages such as its higher dimensional tolerance and less sensitivity to the frequency deviation and cell-to-cell phase deviation [Knapp *et al.* (1965), Knapp *et al.* (1968), Nepal *et al.* (2001), Schächter (2011)].

The working principle of the reltron is similar to that of the klystron, such as the RF interaction cavities converts a continuous electron beam originating from a cathode into discrete electron bunches (i.e. these electron bunches are formed due to velocity modulation), and then the RF power extracted from these electron bunches using a set of output cavities. However, reltron's bunching mechanism differs from klystron, i.e. reltron is based on dual velocity modulation rather than single velocity modulation, and also uses post-acceleration techniques whereas in klystron no such technique is used. The concept of re-acceleration of electron bunches was first introduced in klystron, in which electron bunches are formed by the RF gap fields (inside the RF interaction cavity), and then these electrons were further accelerated with the help of external DC voltages [Hefni (1964)]. This re-acceleration technique was also known as voltage stepping [Marder *et al.* (1992)]. In the post-acceleration technique, a high voltage DC pulse is applied in the post-acceleration region due to which the electron bunches emanating from the RF interaction cavity are accelerated at the relativistic velocity, allowing more kinetic energy is available in these electron bunches for RF conversion. This post-acceleration technique enhances the efficiency of the reltron oscillator by reducing the relative kinetic spread between the electrons present in the electron bunches [Miller *et al.* (1992)].

1.5.1. Literature Review

A highly efficient reltron was experimentally reported by Titan Advanced Innovative Technologies of Albuquerque, NM in the year 1992. The initial experimental results showed that for L-band with the applied DC input voltage of 800 kV and an average input beam current of 1.2 kA the device generates a peak power of >400 MW with the peak conversion efficiency of ≥50%. The total RF energy per pulse for 375 MW peak RF power was 84 J. The stainless steel screens or grids used within the RF interaction cavity were used with 95% transparency. For the S-band, the device generated a peak RF power of 235 MW with a peak conversion efficiency of ~40% when the DC input voltage of 850 kV and an average input beam current of 750 A was applied [Miller *et al.* (1992)].

In the year 1994, the experiment on the progress of reltron was reported. Miller *et al.* reported the analytical model for the rectangular extraction cavity to optimize the extraction of the RF power and obtained a frequency tunning ability in the device by physically deforming the RF interaction cavity by plungers and tunning screws. This tuning feature was built outside the Marx generator tank to achieve this frequency tunability without disassembling the tube or losing the vacuum. For the L-band, a peak RF power of 600 MW and an RF energy per pulse >200 J were obtained, whereas the tunable version of reltron was reported in the S-band. The tunable version of the reltron was capable to generate the peak RF power of >350 MW and the conversion efficiency ~50%. In achieving the ± 5% frequency tunability from the center frequency of the reltron, the peak RF output power was reduced by about 3 dB and this fall in power can be minimized by increasing the injector voltage. They also demonstrate the multiple frequency operation by using an S-band output cavity with an L-band reltron [Miller *et al*. (1994)].

Miller *et al*. also discussed experimental results and theoretical design considerations of the reltron for three specific issues: long pulse operation, extended frequency operation, and extended lifetime designs. For long pulse operation, they achieved a pulse duration of more than one microsecond, with energy per pulse >150 J in L-band. They also developed an HPM effects testing system based on reltron which generates repetitive high-power pulses in the frequency range of 0.7─11 GHz. Finally, they developed a new variant of reltron which uses thermionic cathodes, ceramic insulators, and grid-less RF interaction cavity for long pulse and extended lifetime operation at reasonably high average power levels (>100 kW) [Miller *et al*. (1995)].

Miller discussed the pulse shortening issue in the reltron tube and the effect of pulse shortening due to the materials used in construction, cathode material, vacuum pressure, designing the issue of reltron, and the conditioning process. He used the conventional fabrication methods incorporating the thermionic cathode for electron emission, ceramic insulators, and brazed connexion capable of operating at high-temperature to increase the RF energy per pulse [Miller (1996)].

Miller reported an experimental study on the repetitive operation of the reltron source. The repetitive operation in thermionic emissive-based reltron was limited by the power supply and/or cooling system while in the explosive emission-based reltron it was limited by the rise of vacuum pressure i.e. if the pressure rise above the 10^{-4} torr the voltage pulse was significantly degraded and it limits the device operation. They also developed a mathematical model that describes this phenomenon. He also suggested CsI-coated graphite cathode in place of velvet cathode as a potential HPM cathode material because it generates less gas than the velvet cathode [Miller (1997)].

Miller discussed the operation of the reltron source and mentioned several high voltage DC generators used to drive the reltron. The conventional Marx generator with crowbar switch has been used for single pulse operation while for repetition rates up to a few tens of Hertz PFN Marx pulsers have been used. The thyratron-switched, transformer-based generator has been used when the repetition rate over a few tens of Hertz was required [Miller (1997)].

Ding has given the analytical description of the RF generation process in the reltron and explained the physical significance of the beam bunching in the RF interaction cavity and the extraction section [Ding (1997)].

Miller also discussed the two major points, which were mainly responsible for the pulse shortening issue in the reltron tube. First, the high field stress in the cavities is caused by a relatively good vacuum condition (10^{-5} torr), and second, when the vacuum pressure of the tube increases up to 10^{-4} torr range, it limits the repetition pulse operation. He observed that the electric field stress should maintain below the threshold limit of 150 kV/cm to avoid the electric breakdown in the RF interaction cavity [Miller (1998)].

Choi *et al.* reported the low operating voltage reltron with its design and initial operating characteristics [Choi *et al.* (2001)]. Choi and Schamiloglu reported a study on the pulse power system of the low operating voltage reltron developed at UNM [Choi and Schamiloglu (2002)].

Kim *et al.* reported the simulation study of S-band grid-less reltron using a commercially available MAGIC-3D software. With a typically selected beam parameter i.e. cathode voltage of 120 kV, beam current of 80 A, and post-acceleration voltage of 800 kV, the simulation predicts that the modeled device can generate 38.3 MW of RF power with the pulse width of 200 ns and the device efficiency 52.7%. For the electron beam confinement in the device, they applied an external DC magnetic field of 1.4 kG. [Kim *et al.* (2009)].

Soh *et al.* has reported an analytical model to produce a maximum of 120 kV DC potential by utilizing a double bipolar juncture 396 J Marx generator. The resultant DC pulse was approximately 1—4 μs with less than 0.25 μs rise time. The MAGIC simulation predicted an average peak current of 1.2 kA, while the analysis provided a peak current of 1.38 kA [Soh *et al.* (2009)]. Soh *et al.* also performed a circuit analysis of the reltron's RF interaction cavity. They designed and simulated the RF interaction cavity of the reltron using MAGIC-3D EM software and obtained that the $\pi/2$ and π modes resonate at 2.70 GHz and 3.29 GHz, respectively [Soh *et al.* (2010)]. Further, Soh *et al.* reported a dual cavity reltron to improve the RF output power of the device [Soh *et al.* (2011)]. Soh *et al.* reported a dual-mode reltron that is capable of generating two modes simultaneously or separately. With a 1 ns rise time step supply, the anode-cathode is driven by 175 kV while the post-acceleration region is driven by 500 kV. With TM_{010} mode excitation, they have generated 81 MW microwave power with 23% efficiency and with TM_{110} mode 74 MW microwave power with 17% efficiency. By exciting both modes simultaneously, they were able to generate 128 MW RF power with 35% efficiency [Soh *et al.* (2012)].

Mahto and Jain, gave a brief device description, the operating principle, and define the significance of each sub-assembly of the reltron. The relationship between the induced gap voltage in the first grid spacing and the return current due to the formation of the virtual cathode in the second grid spacing was explained with the help of an equivalent circuit approach. A mathematical model for the sustained oscillation condition is described to obtain the self-oscillation condition of the device as well as the oscillation range [Mahto and Jain (2016)]. Mahto and Jain calculated the start oscillation condition for the gridded reltron and discussed its design methodology in detail. They also reported a simulation study of gridded reltron using commercial 3D particle-in-cell (PIC) code CST Particle Studio. Also, the effect of cathode voltage and the post-acceleration voltage on the performance of the device was explored [Mahto and Jain (2016)]. Mahto and Jain calculated the electric field responsible for the electron beam bunching process in the RF interaction cavity and explained the beam wave interaction process in the reltron. They also explained the process of the transformation of the electron beam velocity modulation into the density modulation is in the RF interaction cavity and analytically calculated the RF energy which was developed in the device [Mahto and Jain (2016)].

Mahto and Jain reported a mechanism of formation of the virtual cathode in the RF interaction cavity in a gridded reltron. The virtual cathode formation is due to the space charge current, and its steady-state electric field distribution was numerically analyzed. In the device, the first virtual cathode was created in the post-acceleration gap, and then the second virtual cathode forms between the first and second grids of the modulation cavity. These two virtual cathodes coexist and cause the creation of a third virtual cathode between the second and third grids. In this condition, only the third virtual cathode remains, and for continuous device oscillation, this process periodically repeats in the device [Mahto and Jain (2017)]. Mahto *et al.* also reported a simulation study of virtual cathode formation in the device. The multistage virtual cathode formation was demonstrated in the gridded reltron through the CST's simulation [Mahto and Jain (2018)].

1.5.2. Classification of Reltron

Reltron is a new kind of relativistic klystron that uses the concept of the post-acceleration technique [Miller *et al.* (1992)]. The development of the reltron begins through the investigation of the klystron-like split cavity oscillator (SCO) [Miller *et al.* (1992)]. Reltron is a promising slow-wave HPM source due to its high efficiency, low design complexity, multiple frequency operation, compact and lightweight. Fig. 1.5. shows the different possible ways to classified the reltron source but commonly it is grouped into two ways (i) gridded reltron or explosive emission-based reltron, and (ii) grid-less reltron or thermionic emission-based reltron [Miller *et al.* (1995)].

(a) *Gridded Reltron*: The gridded reltron uses metal grids in the RF interaction cavity and the RF extraction cavities. The gridded reltron uses an explosive emission cathode for its electron beam. The bunching mechanism is based on virtual cathode formation and it does not require an external DC magnetic field for its proper operation. This device generates high peak RF power with a pulse width of ≤100 ns and having a low repetition rate i.e. ≤10 Hz. After a few shots, the metal grid used in the RF interaction cavity gets burned out and therefore it demands regular maintenance for proper operation [Miller *et al.* (1992), Miller (1998)].

(b) *Grid-less Reltron*: In grid-less reltron uses a metal disc in place of metal grids in the RF interaction cavity. The grid-less reltron uses a thermionic emission cathode for its electron beam. The bunching mechanism is based on velocity modulation and it requires a small external DC magnetic field for its proper operation. This device is well suited for high-average-power applications and the device generates a pulse width of 5 μs and having a high repetition rate i.e. ≥100 Hz. This device does not require regular maintenance like gridded reltron [Miller *et al.* (1995)].

The gridded reltron and the grid-less reltron have many differences such as their electron bunching mechanism, use of the different types of the cathode for the electron beam generation, the geometry of RF interaction cavity or modulating cavity, external magnetic field requirement, pulse repetition rate (PRR), and required operating voltage. (i) *Electron bunching:* The bunching of electrons in a gridded reltron is caused by the formation of a virtual cathode, while in grid-less reltron is due to velocity modulation of the electron beam. (ii) *Cathode for electron beam generation:* For the electron beams, the gridded reltron is based on an explosive emission cathode, while the grid-less reltron is based on the thermionic cathode. (iii) *The geometry of the RF interaction cavity*: The RF interaction cavity i.e. side coupled-cavity (SCC) is used in both types of reltron but the major difference is that the gridded reltron uses the metal grids in SCC while the grid-less reltron uses the metal disc in SCC. (iv) *External magnetic field*: The gridded reltron operates with a self-magnetic insulation condition therefore it does not require any external magnetic field because for its operation while the grid-less reltron required a small external DC magnetic field for its operation. (v) *Pulse repetition rate (PRR):* The reported PRR of the gridded reltron and grid-less reltron is 10 Hz and 100 Hz, respectively. (vi) *Operating voltage*: For the operation, the gridded reltron demands a high voltage supply as compared to the grid-less reltron [Miller *et al.* (1992), Miller *et al.* (1995)].

Each type of reltron has its advantages and disadvantages as well. The main advantage of the gridded reltron is that it does not require any external magnetic field for its operation and this makes the device lighter. While the major constraint associated with the gridded reltron is the formation of plasma which limits the PRR and introduces a pulse shortening phenomenon within the device. The intense relativistic electron beam (IREB) generated through the explosive emissive cathode when collide with the metal grid used in the RF interaction cavity generates plasma in the vicinity of the metal grid which is the main cause of pulse shortening and also limits the PRR of the device [Miller (1998)]. The other constraint associated with the gridded reltron is the use of metal grids in its RF interaction cavity that is burned out after a few shots, requires replacement of grids at regular time intervals for its proper functioning. For the grid-less reltron, its major advantages are its long RF pulse generation and high PRR which is around 100 Hz. Grid-less reltron achieves high PRR and long RF pulse due to the use of non-explosive cathodes i.e. thermionic cathode, and the use of metal discs in place of metal grids, which reduces

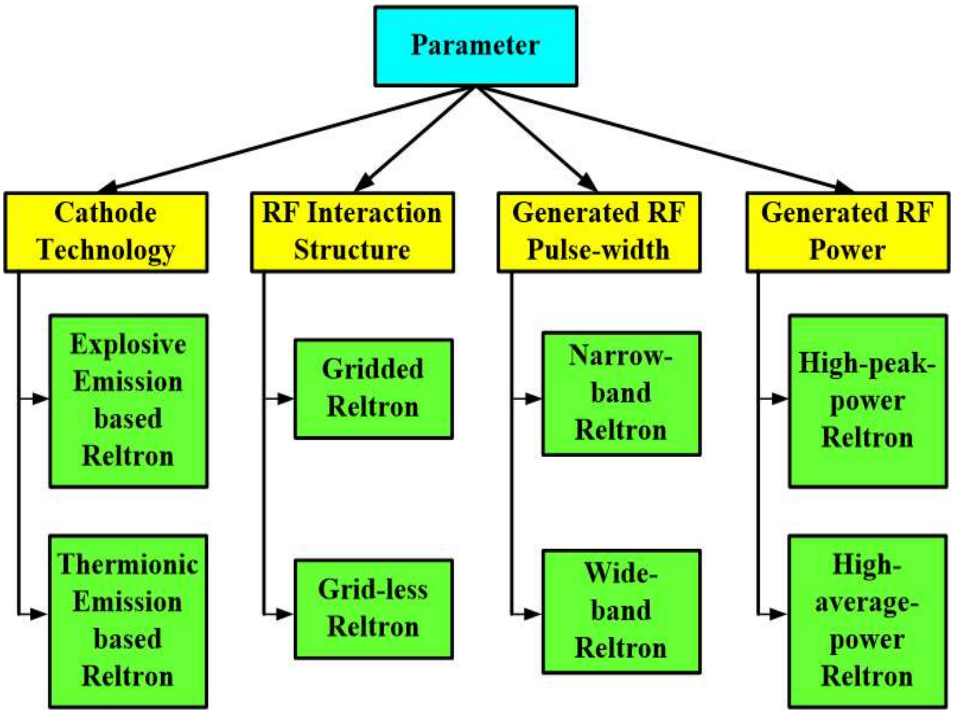

Figure 1.5: Different possible ways to classify the reltron source.

the possibility of plasma formation inside the device. The life of the grid-less reltron is more than that of the gridded reltron [Miller *et al.* (1995)]. Despite all these advantages, the major disadvantage associated with a grid-less reltron is the use of an external DC magnetic field for its operation that makes the device a little bit bulkier as compared to the gridded reltron. Another disadvantage of the grid-less reltron is its low RF output power generation.

1.5.3. Key Features

Despite its high efficiency and large stable tuning range, the reltron has many other unique features such as [Miller *et al.* (1992), Miller *et al.* (1994), Barker and Schamiloglu (2001), Benford *et al.* (2007)]:

- The distance required to create the electron bunches is quite short, which makes the tube very compact.
- To focus the electron beam, the gridded reltron does not require an external magnetic field while the grid-less reltron requires a very small magnetic field that is fulfilled by using permanent magnets.
- The operation mode of the device is TM_{01} mode while RF output power is extracted in TE_{10} mode. Due to this feature of reltron, there is no demand for any external mode converter which increases the overall efficiency of the device.
- The excellent beam bunching present in the device allows RF power extraction at multiple frequencies by using different RF extraction cavities of different frequency bands.

- The post-acceleration technique in the device helps in the formation of more tight electron bunches by reducing the kinetic energy spread between the electrons present in the electron bunches and it also increases the velocity of these electron bunches to approximate velocity of light due to which more kinetic energy is available for RF conversion in the extraction cavity.

1.5.4. Applications

- To study the HPM effects on the electronic components or device.
- Food irradiation.
- Material Processing.
- A directed-energy weapon (DEW).
- Other possible applications such as cargo inspection, imaging, radar, plasma science, and the medical domain.

1.6. Motivation and Research Objective

Over the past few decades, many research studies on high-peak-power or single-shot or low-repetition microwave sources have been published, while very few research work on high-average-power or high-energy, high-repetition microwave sources have been reported. This existing huge research difference, motivate the author to work on such type of devices. In addition, such devices also have many potential applications in various domains such as defense (electronic warfare, directed-energy weapon, jammer, imaging, high power radar, study the effect of HPM on the survivability/ vulnerability of electronic component or devices), civilian (food irradiation, material processing, cargo inspection), and scientific and medical, also attracts the author to research on the high-average-power HPM source.

The definition of research objectives for the doctoral thesis is through a cycle that includes a concise literature survey and identification of research areas in the domain of HPM sources. Due to its strategic nature, limited literature is available on the grid-less reltron and a concise description of the device is not underlined anywhere. Therefore, the main objective of this research work is to clearly explain the basic principles of its operation, to reduce the design complexity related to its key components, and to remove the existing flaws in the available literature. The previously reported literature on the grid-less reltron i.e. experimental, theoretical, and simulation studies, has been used to develop the basic concept of the device. The main objective of this thesis is to further enrich the knowledge of the device by contributing some fundamental work on the device so that researchers and developers can understand the physics of the device. To achieve these objectives, firstly the behavior of the RF interaction structure (i.e. SCC) is investigated in the presence and absence of the electron beam for a better understanding of the device's mechanism. The working principle of the device, its theoretical analysis, a simulation study of its key component i.e. RF interaction cavity with the comprehensive simulation study of grid-less reltron have been performed and finally, a new variant of grid-less reltron has been proposed to enhance the RF output power of the device.

1.7. Organization of the Thesis

The grid-less reltron is the newest member in the HPM family and it attracts the researchers due to its high efficiency, compact size, multiple frequency operation, frequency stability, frequency tunability, and long pulse operation with high PRR. Since the grid-less reltron belong to the category of high-average power HPM source and due to its several potential applications in various domains, it is essential to develop a better understanding of its key components and device physics. In this thesis, the RF interaction cavity of the grid-less reltron (i.e. side coupled-cavity (SCC)) has been studied through various analytical approaches as well as EM simulation software. Also, a comprehensive simulation study of grid-less reltron has been performed to investigate the structural and electrical parameter dependency. Finally, a new variant of grid-less reltron has been proposed to improve the RF output power of the device and investigate its RF behavior for the different possible electrical specifications through simulation. Accordingly, the thesis is divided into six chapters, as follows.

In chapter 1, the origin of HPM and its basic definition has been discussed along with the various methods of classifying the HPM sources. With a detailed literature review of reltron, various methods of classifying it are also presented. Several potential applications of Reltron and its unique advantages are also listed in this chapter. Finally, the motivation and research objectives of the research study and the plan and scope of the thesis are described.

In chapter 2, the resonating frequency associated with the SCC has been theoretically derived with the help of an equivalent circuit approach. This research study focuses on estimating the coefficient of the magnetic coupling factor in terms of its structural parameters, which have so far been experimentally calculated. An empirical formula has been proposed to calculate the frequency associated with the fundamental resonance mode that includes the effect of the magnetic-coupling factor, which has not been considered in the previously reported researches. To validate this research study, firstly the SCC is designed and simulated with the help of "CST Studio Suite" and results of the proposed empirical formula are compared with the simulation results.

In chapter 3, the electromagnetic (EM) behavior of the SCC structure is investigated in the existence of an electron beam using a field matching approach for the transverse magnetic $\left(TM_{01}\right)$ mode. The Vlasov-Maxwell's equation is used to analyze the region in which an electron beam has present. Due to its potential application as a beam wave interaction structure in transit time oscillator, backward wave oscillator, and traveling wave tube its dispersion relation has been obtained by considering the effect of all harmonics present within this structure. The analysis is further extended to assess the operating frequency and temporal growth of the structure. Also, the effect of the different beam parameters on the temporal growth rate behavior has been analyzed. Due to the unavailability of previously reported experimentally and theoretical literature, the performed theoretical analysis is validated for the special case (i.e. $r_e = 0$) by comparing the analytical dispersion curve with the simulated dispersion curve.

In chapter 4, the design and simulation study of a highly efficient grid-less reltron based on the thermionic emissive cathode is described in detail. Initially, the design process of the entire grid-less reltron device is explained, and its RF interaction cavity model is then designed with the help of "CST Studio Suite". The electromagnetic behavior of the designed RF interaction cavity is investigated with the help of an eigenmode solver and frequency-domain solver. Also, a comprehensive simulation has been performed to explore the structural dependency of the RF interaction cavity on the frequency of the fundamental resonance mode. To find out the RF behavior of the designed device, the device is simulated with the help of a particle-in-cell (PIC) solver. An electrical parametric analysis has been performed to evaluate the performance of the modeled device. For validation, the simulated results are compared with the previously reported experimental results, and it is found that the relative error is within 5%.

In chapter 5, a new variant of the reltron oscillator (i.e. grid-less reltron with explosive emissive cathode) is proposed to get high power, a long pulse, and high PRR. The electric field distribution and resonant frequency corresponding to the different resonance modes of the SCC are obtained using the eigenmode solver and the frequency domain solver, respectively. To achieve its RF behavior, the proposed variant is modeled and simulated using a PIC solver. Also, the effect of different electrical parametric on the RF output power, efficiency, and RF pulse-width are investigated. The present study compares the simulation and experimental results of gridded and grid-less reltron to find out the achievements of the proposed reltron. The proposed variant of reltron demands a lower operating supply than the gridded reltron and produces approximately the same peak RF output power, but the generated RF pulse width is 10 times higher than the gridded reltron. While in comparison with the grid-less reltron, it generates an RF peak power 10 times higher but the generated RF pulse width is 1/5 times lower.

In Chapter 6, the research work performed in the thesis is firstly summarized and then the major findings of the research work and their significance are discussed. Future scope and extension work is outlined.